Influence of the Metal Cross-Linking on the Dielectric, Mechanical, and Thermal Properties of a Liquid Crystalline Polyazomethine

J. A. Puértolas*

Departamento Ciencia de Materiales, Centro Politécnico Superior, Universidad de Zaragoza, María de Luna 3, 50015 Zaragoza, Spain

E. Carod

Departamento Ingeniería Eléctrica, Centro Politécnico Superior, Universidad de Zaragoza, 50015 Zaragoza, Spain

R. Díaz-Calleja

Departamento Termodinámica Aplicada, Escuela Superior de Ingenieros Industriales, Universidad Politércnica de Valencia, 46071 Valencia, Spain

P. Cerrada, L. Oriol, M. Piñol, and J. L. Serrano

Química Orgánica, Instituto de Ciencia de Materiales de Aragón, Universidad de Zaragoza−CSIC, 50009 Zaragoza, Spain

Received July 26, 1996; Revised Manuscript Received November 11, 1996[⊗]

ABSTRACT: Cross-linked polymeric materials have been synthesized by copper(II) complexation of a semiflexible main-chain liquid crystalline polyazomethine. The influence of the copper(II) cross-linking density on the thermal properties has been studied by DSC. The relaxation behavior of both the parent polymer and the complexed polymers has been investigated by dielectric spectroscopy and dynamic mechanical measurements. The parent compound exhibits three relaxations (denoted by α, β, and γ), together with a conductive process at low frequency. The relaxations have been associated with the glass transition (α), rotational motions located in the rigid mesogenic core (β), and local motions of the decamethylene flexible spacer (γ). Semiempirical calculations have been carried out in order to evaluate the rotational energy barriers which can account for the β process. The influence of the degree of cross-linking on the activation energies and on the strength and shape parameters has also been studied in the copper(II)-complexed polymers.

Introduction

Polyazomethines or Schiff base polymers may exhibit a variety of interesting physical properties such as electronic, optoelectronic, nonlinear optical, or liquid crystalline properties that make this kind of polymer particularly interesting in materials science.[1] This type of material has drawbacks such as low solubility in common organic solvents and high melting temperature, which makes its processing difficult. However, films or fibers of their anisotropic melts have been reported and fibers drawn from the nematic melt of aromatic polyazomethines exhibit particularly excellent mechanical properties.[2]

We have previously described a series of polyazomethines whose structural design includes a decamethylene flexible spacer connecting rigid units and functional hydroxyl groups have been incorporated in the *ortho* position of the azomethine bond.[3] The hydroxyl groups form hydrogen bonds with the nitrogen atom, causing an increase in the anisotropy of the electronic polarizability and the backbone planarity, which favors the appearance of mesomorphic phases.[4] In spite of the presence of a decamethylene flexible spacer in the polymeric chain, the fibers extruded from the nematic melt of these polyazomethines show good mechanical properties.[5] Furthermore, the hydroxyl groups allow the chemical modification of the polyazomethines, which may lead to cross-linking and an improvement in the mechanical properties of fibers, especially in the direction perpendicular to the fiber axis. An interesting way to modify these polymeric materials is by complexation with metal ions. Metal-complexed Schiff base polymers have been described which exhibit a wide variety of properties such as luminescence[6] or catalytic properties.[7] We have recently reported the metal modification of hydroxy-functionalized polyazomethines to yield different series of metal-containing liquid crystal polymers (LCPs) or metallomesogenic polymers.[8] These metallomesogenic polymers may be considered as hybrid materials which combine the anisotropic properties of liquid crystals, the physical properties of metal atoms (e.g., color, magnetism, catalytic properties, and a high electronic polarizability), and the processing properties of polymers.[9]

In this article, we present a study of the dynamic molecular features of copper(II)-complexed polymers derived from the parent polyazomethine shown in Figure 1 (denoted DMB), as well as the dependence of the thermal properties on the metal complexation. This complexation gives rise to cross-linking of polymeric chains, as confirmed in previous papers.[8] Most of the studies on correlations between relaxation processes and motions of dipolar groups on LCPs deal with organic LCPs, especially side-chain polymeric systems.[10] However, only a few studies have been reported concerning metal-containing LCPs.[11−13] As far as we know, this is the first study regarding the dynamic molecular properties of metal-coordinated LCPs in which the metal complex acts as the cross-linker of the polymeric chains.

* To whom correspondence should be addressed. Phone +34-76-761958, Fax +34-76-761957, e-mail jap@mcps.unizar.es.

[⊗] Abstract published in *Advance ACS Abstracts,* January 15, 1997.

S0024-9297(96)01119-9 CCC: $14.00

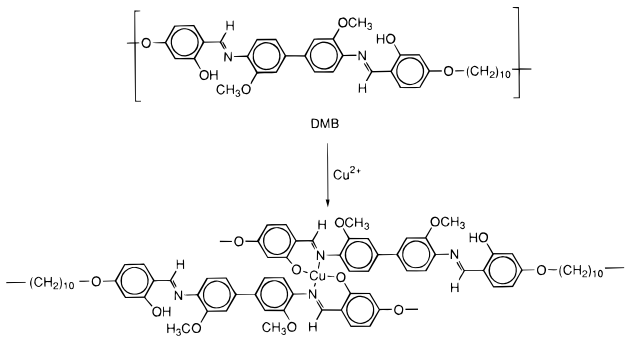

Figure 1. Repeating unit of the parent polyazomethine DMB and schematic representation of cross-links introduced by copper(II) complexation.

Table 1. Characterization Data of the Parent and Copper(II)-Complexed Polyazomethines

	% Cu			
polymer	calcd	found	introduced[a]	C=N str (cm^{-1})
DMB				1618
DMB-5	5.78	2.76	48	1618
DMB-10	10.72	4.84	45	1618
DMB-20	20.74	9.50	46	1616

[a] % introduced = (% found/% calcd) × 100.

The relaxation behavior has been investigated by dielectric relaxation spectroscopy and dynamic mechanical measurements in the parent polymer, DMB, in terms of the temperature and frequency dependencies of the α process and the secondary processes. In both cases, we have investigated the influence of the copper(II) cross-linking density on the magnitude, temperature, and shape parameter of the relaxations. The activation energy for the sub-glass transitions was calculated from the frequency dependence of the relaxation in each compound in the series. Computational modeling was carried out on the parent polymer in order to determine the possible molecular motions that could contribute to the β process.

Experimental Section

Materials. The parent polyazomethine, DMB, was synthesized from 1,10-bis[(4-formyl-3-hydroxyphenyl)oxy]decane and 3,3′-dimethoxybenzidine, which was recrystallized from ethyl acetate−hexane prior to use, according to the procedure described previously.[3] Yield: 81%. Anal. Calcd: C, 73.30; H, 6.75; N, 4.50. Found: C, 72.81; H, 7.05; N, 4.53. η_{inh} (0.5 g/dL in methanesulfonic acid at 40 °C): 0.98. The parent polyazomethine DMB has good film- and fiber-forming properties, which indicates that the molecular weight is reasonably high. On the other hand, the molecular weight of this type of polymer can be increased by postpolymerization reactions at temperatures close to or above the melting transition.[14]

The metal functionalization of the polyazomethines was carried out by addition of a solution of copper(II) acetate to a suspension of the parent polymer in 1,4-dioxane according to the procedure described elsewhere.[8] The percentage of copper(II) introduced is about 50% of the total amount used in the synthesis. A change in the coloration of the polyazomethine is detected upon copper(II) complexation. The polyazomethine has a yellow color, which darkens to give a dark yellow to brownish color on increasing the copper(II) content.

Techniques. Elemental analyses were carried out using a Perkin-Elmer 240C microanalyzer. FTIR spectra were performed using KBr disks on a Perkin-Elmer FTIR 1600. The copper content was determined by inductively coupled plasma atomic emission spectroscopy using a Perkin-Elmer P-40 spectrometer. Table 1 shows the characterization data for the parent and metal-chelated polyazomethines.

The mesogenic behavior of the polymers was studied by optical microscopy using a Nikon polarizing microscope fitted with a Mettler FP-82 hot stage and a Mettler FP-80 control unit. A Perkin-Elmer DSC-7 was used to determine the thermal transitions, which were read at the maximum of the peaks. Glass transition temperatures were taken as the midpoint of the baseline jump. Both transition temperatures and enthalpy changes were determined using indium and tin as calibration standards. Simultaneous thermogravimetric and differential thermal analysis was performed using an STD 2960 simultaneous TGA−DTA TA instrument at a rate of 10° C/min under a nitrogen atmosphere.

Dielectric measurements were performed using a dielectric spectrometry setup (Novocontrol BDS4000), which includes a two-terminal dielectric cell, a frequency response analyzer (Solartron 1250), and a high-impedance preamplifier of variable gain. The complex dielectric constant was obtained by sweeping the frequency in the range 0.04 Hz to 1 MHz at different stabilized temperatures by heating from −150 to +150 °C in temperature steps of 7 °C. The sample was held between the condenser plates (golden brass circular electrodes, diameter 12 mm) with the aid of a glass-reinforced PTFE annular ring spacer (60 μm thickness and internal diameter 7 mm).

Dynamic mechanical measurements were carried out using a Rheometrics DMTA Mark II apparatus in bending on prismatic test specimens of area 1 × 10 mm^2 sintered from the powdered compound heated to a temperature above its melting point and cooled down at a moderate rate. A double-cantilever technique was used when a large amount of sample was available. However, a single-cantilever technique was used when either the amount of sample available was insufficient or the mechanical behavior proved to be too fragile. Heating runs were made at a rate of 1 °C min^{-1} from −140 °C to approximate 20 °C above the glass transition. The frequencies employed were 0.1, 0.3, 1.3, and 10 Hz.

Table 2. Thermal Stability and Thermal Transition Data of the Parent and Copper(II)-Complexed Polyazomethines

			DSC, 1st heating[a]		DSC, 2nd heating[a]	
polymer	TGA (°C)[b]	DTG (°C)[c]	T_g (°C)	T_m (°C)	T_g (°C)	T_m (°C)
DMB	364	380, 438		195	57	193
DMB-5	360	373, 411	49	187	66	185
DMB-10	355	370, 439	47	193	71	
DMB-20	356	371, 410		144, 158	74	

[a] Scanning rate = 10 °C/min. [b] Onset of the decomposition curve. [c] Differential thermogravimetric analysis.

Results

Thermal Measurements. Table 2 shows the data corresponding to TGA−DTA and DSC measurements of the parent and metal-complexed polyazomethines. The thermal stability of the parent and modified polyazomethines was tested by simultaneous TGA−DTA measurements under a nitrogen atmosphere. All samples exhibited weight loss at temperatures above 350 °C. Weight loss was not detected at lower temperatures. Furthermore, the DTA traces confirm that significant thermal decomposition of the samples occurs with weight loss since there was a concordance between the TGA and DTA decomposition temperatures. The introduction of copper(II) led to a slight decrease in the onset temperature of degradation. The relatively good thermal stability of the copper(II)-modified polyazomethines led us to consider the possibility of processing these partially metal cross-linked polymers from the nematic melt provided that the viscosity of the mesophase was adequate.

The parent polymer is a semicrystalline polymer which shows a glass transition at 57 °C and a melting transition into a mesomorphic melt at about 190 °C. The isotropization transition occurs above 325 °C, detected by optical microscopy, but it could not be clearly

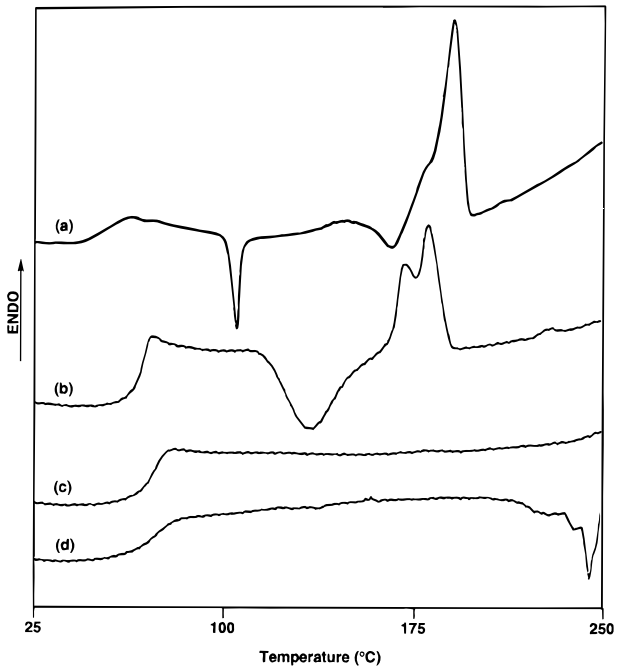

Figure 2. DSC traces corresponding to the second heating run (scan rate = 10 °C/min) of (a) DMB, (b) DMB-5, (c) DMB-10, and (d) DMB-20.

established by DSC because decomposition of the sample takes place simultaneously. The mesophase is identified as nematic by its texture observed by polarizing optical microscopy. However, on annealing the sample at the mesophase temperature for several hours, a change can be observed as the nematic mesophase becomes smectic C. This change in mesophase type was confirmed by X-ray diffraction and reported elsewhere.[15]

Some differences are observed in the DSC traces of copper(II)-complexed polymers in comparison with the parent polymer. Crystallization was not observed on cooling the anisotropic melt of the copper(II) polymers, which form anisotropic glasses. Figure 2 shows the second heating scans of both the parent and the modified polymers. In the case of copper-containing polymers, a glass transition is observed but no further peaks were detected, except in the case of DBM-5. This polymer displayed a cold crystallization above the T_g and a melting transition at temperatures similar to those in the parent polymer. At high temperatures some evidence of thermal instabilities was detected by DSC, especially in polymers with a higher copper content. Furthermore, an increase in the T_g is observed when the metal content increases, as a consequence of the higher degree of cross-linking.

Due to the metal cross-linking, a modification of the mesogenic properties of the parent polymer is expected as the decrease in the molecular mobility around the metal centers must affect the viscosity of the anisotropic melt. For high metal contents, nonfusible cross-linked materials must be expected. Thus, the identification of the nematic nature of the mesophase of these modified polymers is difficult due to the high viscosity of the nematic melts. In fact, this high viscosity hinders the appearance of typical nematic textures. Despite this high viscosity, the textures can be assigned as nematic by comparison with textures of nematic metallomesogenic polymers previously synthesized in our laboratory.[16] The isothermal evolution of the nematic mesophase into a smectic phase observed for the parent polymer could only be observed in samples of DMB-5. Furthermore, for these metal-complexed polymers, the

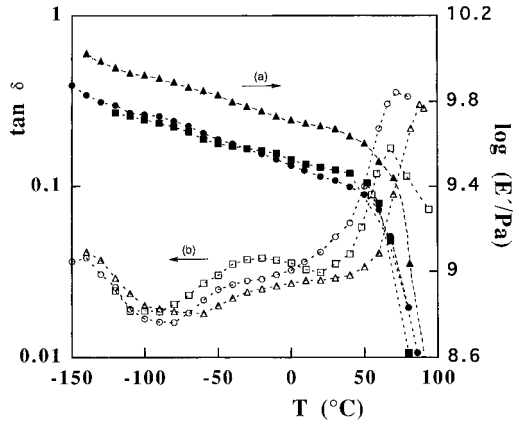

Figure 3. Thermal dependence of (a) log E' (full symbols) and (b) tan δ (open symbols) at 1 Hz in the polymers DMB (□), DMB-5 (○), and DMB-10 (△).

transition into the isotropic molten state was not observed because the samples decomposed before the isotropization takes place.

Dynamic Mechanical Measurements. Heating scans were performed for the parent polymer and complexed polymers, except for DMB-20, in which the extremely high viscosity of the sample precluded the preparation of an adequate test specimen. The thermal variations of the storage modulus, E', and the loss tangent, tan δ, obtained in isochronal conditions ($\nu = 1$ Hz) for the three compounds are depicted in Figure 3. Two relaxation processes can be observed for all the compounds at around −140 and −20 °C, which are respectively assigned as γ and β relaxations. At higher temperatures, about 70 °C, the data for E' and tan δ indicate an α relaxation associated with the glass transition.

Although the γ relaxation process is only partially observed, it seems that this relaxation remains constant for both the parent and copper(II)-cross-linked polymers. A value for the activation energy of this secondary relaxation can be estimated for polymer DMB-5, which exhibits a maximum for tan δ in the measured temperature range (in particular at −140 °C). For this polymer, and within the framework of the Eyring behavior for the dependence of frequency on temperature,[17] given by eq 1 (where k and h are the Boltzmann and Planck constants, respectively, and f is the frequency), the minimum of the activation energy provides a value of 7.4 kcal/mol at 1 Hz for the γ relaxation process.

$$E_a = RT\left(1 + \ln \frac{kT}{2\pi hf}\right) \qquad (1)$$

As regards the β process in the parent polymer DMB, an Arrhenius representation of the frequency versus the temperature maximum (isochronal basis) gives a straight line. The value of the molar activation energy obtained from the slope is $E_a = 19.5 \pm 0.5$ kcal/mol. For copper(II)-cross-linked polymers, an increase in the copper content gives rise to a decrease in the strength of the β relaxation as well as a broadening of the relaxation. The maximum in tan δ seems to shift toward higher temperatures and overlaps with the α relaxation, which hinders an Arrhenius analysis.

The α relaxation associated with the glass transition is more pronounced than the γ or β relaxations. The temperature region in which this relaxation is observed shifts to higher temperatures as the cross-linking density increases.

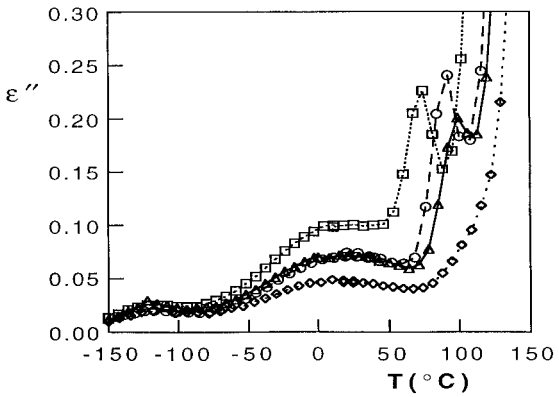

Figure 4. Temperature dependence of the dielectric loss factor, $\epsilon''(T)$, at 1 kHz in the polymers DMB (□), DMB-5 (○), DMB-10 (△), and DMB-20 (◊).

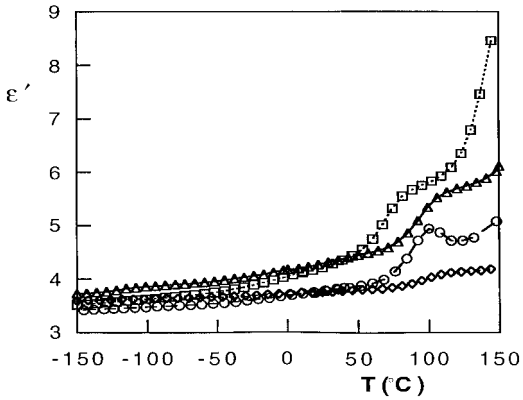

Figure 5. Temperature dependence of the real part of the dielectric constant, $\epsilon'(T)$, at 1 kHz for the polymers DMB (□), DMB-5 (○), DMB-10 (△), and DMB-20 (◊).

Dielectric Measurements. The dielectric measurements provide information about $\epsilon^*(\omega,T)$ for all the polymers in the temperature and frequency range of interest. Figure 4 shows the thermal variation of the dielectric loss factor, $\epsilon''(T)$, obtained at a frequency of 1 kHz and at different stabilized temperatures. Examination of these results reveals the existence of three relaxations and a conductive process at high temperatures for all polymers. As a consequence of the temperature region where the relaxations appear, and in accordance with the mechanical data, they have been denoted as γ, β, and α processes.

Consideration of $\epsilon''(T)$ shows that the maximum for the γ relaxation appears at about the same temperature (for the same frequency) for both the parent and the copper(II)-complexed derivatives. This trend was also observed in the dynamic mechanical measurements. A similar tendency is observed for the β relaxation. However, in the case of the dielectric measurements, the γ relaxation is weaker in strength and narrower than the β relaxation in comparison with the same relaxations in dynamic mechanical measurements. In the case of the α relaxation, a dependence on the copper(II) cross-linking density can be observed according to DSC and dynamic mechanical measurements.

The results corresponding to the real part of the dielectric constant, $\epsilon'(T)$, are shown in Figure 5. The secondary processes are detected as two small steps. Two effects occur at high temperature. The first is related to the glass transition and the increase in the mobility of the dipolar moieties (α relaxation). The second effect, detected in compounds DMB and DMB-5, consists of the existence of a well in $\epsilon'(T)$ after passing above the T_g at higher frequencies. A possible interpretation could be related to a cold crystallization. The loss of mobility as a consequence of the reduction in the amorphous part could cause a decrease in the value of the dielectric constant in this semicrystalline polymer. This is confirmed by the DSC measurements. Similar behavior was observed in the dielectric study of a metallomesogenic polyester previously reported.[18]

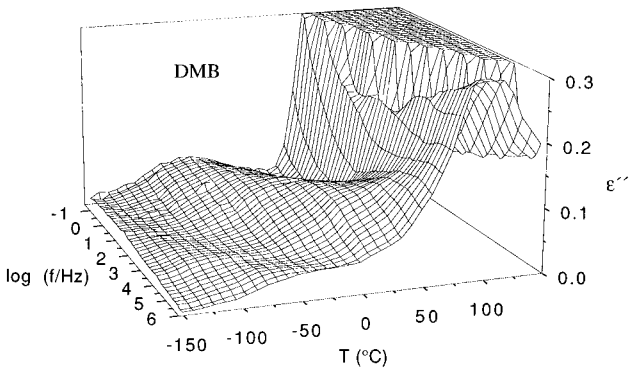

Figure 6. Dielectric loss ϵ'' vs temperature and logarithm of frequency for the polymer DMB.

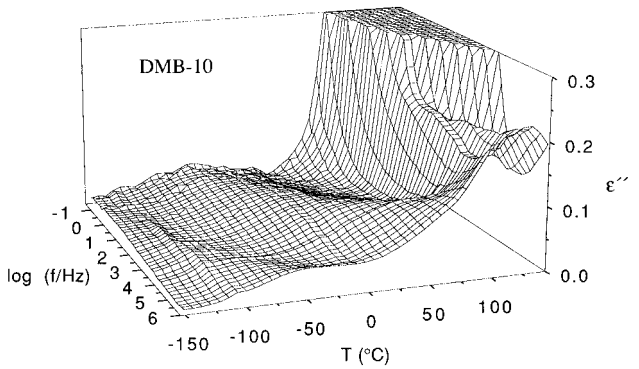

Figure 7. Dielectric loss ϵ'' vs temperature and logarithm of frequency for the polymer DMB-10.

A frequency analysis has been made from the frequency sweep obtained under isothermal conditions. The results of $\epsilon''(\omega,T)$ are shown in Figures 6 and 7 in a typical 3D representation for the parent polymer DMB and polymer DMB-10 as a representative example of the complexed polymers.

The γ and β processes for all of the compounds have been discussed in terms of the Cole−Cole expression that describes the frequency dependence of the dielectric complex constant in the secondary relaxations

$$\epsilon'' = \mathrm{Im}\left(\epsilon_u + \frac{\epsilon_r - \epsilon_u}{1 + (i\omega\tau_0)^{1-\mu}}\right) \qquad (2)$$

in which τ_0 is the relaxation time of the process, μ is a dimensionless parameter related to the width of a relaxation time distribution, and ϵ_u and ϵ_r are the unrelaxed and relaxed values of the dielectric constant, respectively. For the γ and β relaxation processes, the relaxation time, τ_0, fits the temperature according to an Arrhenius behavior $\tau_0 = \tau_\infty \exp(E_a/k_B T)$, where E_a is the activation energy and τ_∞ is the preexponential factor. The values of the molar activation energies for the γ and β processes obtained by fitting the data in the range from −150 to −80 °C and −50 °C to +60 °C are shown in Table 3 together with the values of the relaxation strength, $\Delta\epsilon$, and the shape parameter, μ. A range of values for $\Delta\epsilon$ and μ have been indicated since both parameters are strongly temperature dependent.

Table 3. Activation Energy (E_a), Dielectric Strength ($\Delta\epsilon$), and Shape Parameter (μ) (Fit to Eq 2) for the γ and β Processes of the Parent and the Copper(II)-Complexed Polymers

	γ process			β process		
polymer	E_a (kcal/mol)	$\Delta\epsilon$	μ	E_a (kcal/mol)	$\Delta\epsilon$	μ
DMB	6.2 ± 0.2	0.10−0.12	0.75−0.52	16.4 ± 0.4	0.90−1.10	0.81−0.72
DMB-5	6.5 ± 0.1	0.10−0.11	0.70−0.45	16.1 ± 0.5	0.60−0.70	0.80−0.69
DMB-10	7.2 ± 0.1	0.11−0.14	0.69−0.58	16.6 ± 0.4	0.50−0.80	0.79−0.72
DMB-20	7.2 ± 0.1	0.11−0.13	0.69−0.60	13.3 ± 0.7	0.50−0.60	0.81−0.72

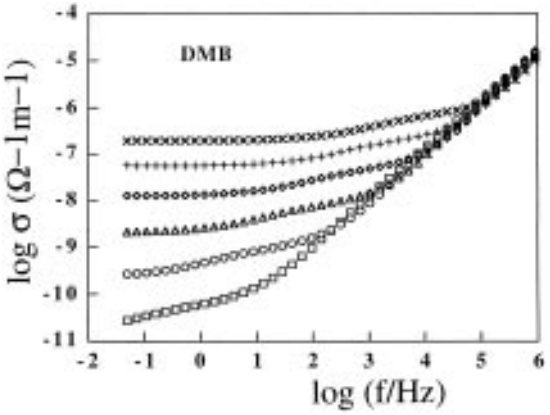

Figure 8. Frequency dependence of the conductivity, $\sigma(\omega)$, for DMB measured at different temperatures above T_g: (□) 74, (○) 86, (△) 102, (◇) 116, (+) 130, and (×) 145 °C.

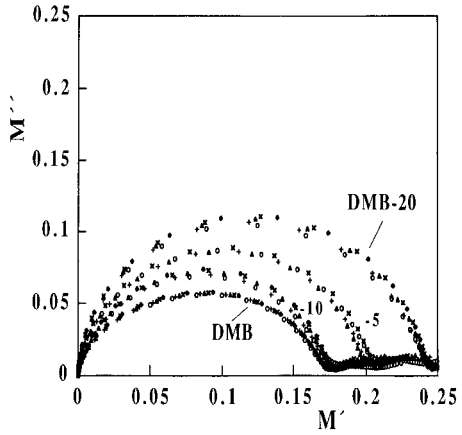

Figure 9. Complex electric plots of M'' vs M' for DMB, DMB-5, DMB-10, and DMB-20 at temperatures above Tg (70−150 °C).

The dynamic behavior of the α relaxation is discussed below since the procedure used to gain information on this relaxation requires careful consideration due to partial masking by other processes.

Discussion

The data corresponding to the isochronal storage modulus, E', obtained from the dynamic mechanical analysis show that the stiffness of the samples is dependent on the copper(II) content. The stiffness of the complexed polymers is higher than that of the parent polymer and increases as the copper(II) content increases due to the higher cross-linking density.

The α relaxation process associated with the glass transition is observed in both the dynamic mechanical and dielectric measurements over a temperature range according to the DSC data. However, in the dielectric study this process is partially overlapped by a low-frequency dispersion behavior, which is clearly observed in the $\epsilon''(\omega,T)$ curves plotted in Figures 6 and 7. In order to separate both effects, this strong dispersion has been studied. One method of analyzing dielectric results in which conductivity effects are significant is the discussion of these effects in terms of the complex conductivity $\sigma^* = \epsilon^*\omega$. In this description, and considering the absence of dipolar relaxations, $\sigma^*(\omega)$ is given by the expression

$$\sigma = \sigma_{dc} + \sigma_{ac}\omega^s \tag{3}$$

where σ_{dc} is the frequency-independent term and ω^s is the Jonscher or "universality class" term,[19] with values of the parameter s between 0 and 1. The results obtained for polymer DMB are depicted in Figure 8. Evidence of a σ_{dc} contribution is observed only at temperatures above the T_g. As far as the ω^s term is concerned, the s values obtained for all the temperatures in the region from 67 to 150 °C are in the range 0.9−1.0.

In addition to the above behavior, the conductivity also reflects the α process, but this is masked by the ω^s contribution. At low frequency and at temperatures above T_g, a substantial separation from σ_{dc} appears, which could indicate the presence of a new relaxation process. In order to clarify the nature of this relaxation, the complex electric modulus representation has been chosen. The relaxation behavior of the electric field in the frequency domain is given by the formula[20]

$$M^*(\omega) = M_\infty \int_0^\infty \Phi(\tau) \frac{i\omega\tau}{1 + i\omega\tau}\, d\tau \tag{4}$$

where τ is electric field relaxation time, $\Phi(\tau)$ the normalized probability function for τ, and M_∞ is the limiting high frequency of the real part of M^*. The complex modulus M^* (calculated from the expression $M^* = 1/\epsilon^*$) is shown in Figure 9 in a complex plot (M'' vs M') for all polymers. The plot shows at low frequency a depressed circular arc for the conductive process with the center located at an angle θ below the real axis. The values of θ deduced from the different compounds vary between 12 and 25°, with compound DMB showing the maximum value.

Figure 10 shows a master curve for the parent polymer obtained from $M''(\omega)$ vs f/f_p, where f_p is the frequency of the maximum in each of the isothermal $M''(\omega)$ curves. The loss peak is symmetrical and the value of the width at half-height is 1.82 decades, higher than the value 1.144 corresponding to the Debye process. For the copper(II)-complexed polymers, master curves having widths of 1.40, 1.38, and 1.35 are obtained for compounds DMB-5, DMB-10, and DMB-20, respectively.

The temperature dependence of f_p is well described by the Williams−Landel−Ferry equation[21]

$$\log \frac{f_p}{f_0} = \frac{C_1(T - T_g)}{C_2 + T - T_g} \tag{5}$$

where T_g is the static glass transition temperature, f_0 is the corresponding relaxation rate, and C_1 and C_2 are fitting parameters. A relaxation rate of around f_0 =

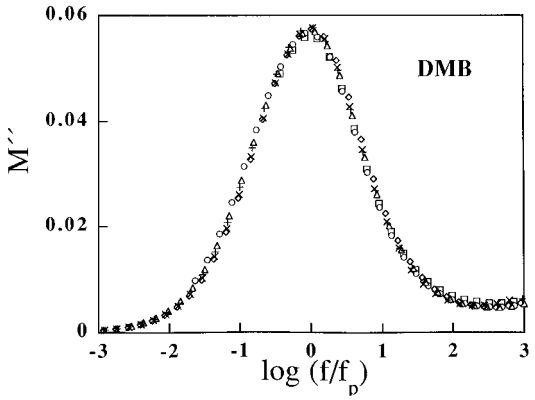

Figure 10. Master curve (M'' vs f/f_p) for the low-frequency relaxation in DMB at temperatures above T_g: (□) 74, (○) 88, (△) 102, (◇) 116, (+) 130, and (×) 145 °C.

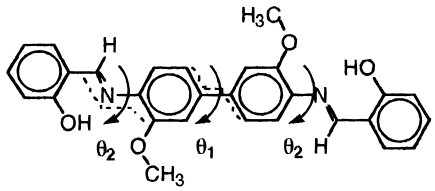

Figure 11. Dihedral angles for rotational motions in the rigid mesogenic core.

0.001 Hz is obtained for all polymers at their corresponding T_g.

In order to study this conductivity process, we have analyzed the data in the framework of an electrical model recently reported in the literature.[22] The application of this model led us to consider that our process is associated with a bulk process rather than an interfacial one. Taking into account the thermal behavior exhibited by the samples, two phenomena might be involved in this process. On the one hand, a cold crystallization could occur above the T_g, although this crystallization is only observed in the DSC traces of compounds DMB and DMB-5. Furthermore, the process can also be observed at relatively high temperatures in the dielectric studies (about 150 °C). On the other hand, the phenomenon might be related to a slow conversion of the nematic phase into a more ordered smectic phase. This change is observed by optical microscopy only when the viscosity of the sample is sufficiently low, as in the case of the parent polymer DMB and the polymer with a low copper(II) content, DMB-5.

Returning to the α process and considering the above-mentioned phenomenon, we have analyzed $\epsilon''(\omega)$ over the whole frequency range on the basis of two Cole−Cole terms (one for the β relaxation and the other for the low-frequency relaxation) and a Havriliak−Negami term for the glass transition and the dc conductivity contribution.[23]

$$\epsilon'' = \mathrm{Im}\left(\epsilon_u + \frac{\epsilon_r - \epsilon_u}{(1 + (i\omega\tau_0)^{1-\mu})^{\delta}}\right) \qquad (6)$$

The δ parameter is a nonsymmetrical shape parameter and the remaining symbols have the same significance as in formula (2). The results show a decrease in the α process intensity with respect to cross-linking. The values of $\Delta\epsilon$, which are temperature dependent, are shown in Table 4.

The temperature dependence of the frequency of the maximum in the isothermal curves follows a Vogel−Fulcher−Tamman−Hesse behavior:

$$f_p = f_0 \exp\left(\frac{B}{T - T_0}\right) \qquad (7)$$

where, due to the limited temperature range and the small number of points for the fit, a fixed value of $f_0 = 10^{13}$ Hz has been assumed. The results are collected in Table 4 and indicate that the apparent activation energy, B, rises as the copper content increases. For the ideal glass transition temperature T_0, with the exception of compound DMB-20, the values follow the same tendency as the glass transition obtained by DSC, with the values being lower than the calorimetric T_g in each case, as reported in other systems.[24, 25]

Table 4. Dielectric Strength ($\Delta\epsilon$), Shape Parameters (μ, δ) (Fit to Eq 6), Activation Parameter, (B), and Ideal Glass Transition Temperature (T_0) (Fit to Eq 7) for the α Process of the Parent and the Copper(II)-Complexed Polymers

polymer	$\Delta\epsilon$	μ	δ	B (K)	T_0 (K)
DMB	1.7−2.2	0.6−0.5	0.4−0.3	643 ± 10	279 ± 1
DMB-5	1.1−1.3	0.6−0.4	0.5−0.3	742 ± 26	288 ± 2
DMB-10	0.7−1.3	0.5−0.3	0.6−0.4	725 ± 66	294 ± 7
DMB-20	0.1−0.3	0.7−0.6	0.5−0.3	865 ± 33	282 ± 3

Concerning the β process, the calculated activation for polymer DMB is 16.4 ± 0.5 kcal/mol (see Table 3), which is smaller than the value obtained from the mechanical measurements, 19.5 ± 0.5 kcal/mol. According to these values, and for the temperature region in which the relaxation appears, we can tentatively attribute this sub-glass process to localized rotational motions in the rigid mesogenic core (see Figure 11), where the hydroxyl groups are involved in relatively strong hydrogen-bonded chelate rings.[26]

Semiempirical calculations using the MOPAC-AM1 program[27] were carried out to ascribe the β relaxation. We first studied the dependence of the potential energy on the dihedral angle θ_1 of the biphenyl unit in the mesogenic core, taking the minimun-energy structure as the initial geometry. The rigid rotation from this minimum-energy structure leads to a rotational energy barrier of about 3.5 kcal/mol when the dihedral angle approaches 0 or 180°. This low value, which is similar to that reported for unsubstituted biphenyl (about 2 kcal/mol),[28] does not account for the experimental results. In order to study the rotational energy barrier as a consequence of the rotation of the dihedral angle θ_2, we selected *N*-(2-methoxyphenyl)salicylaldimine as a model of the mesogenic core. In this case, the calculated rotational barrier was about 13 kcal/mol, with a maximum energy when θ_2 approaches 0°, due to the steric repulsion between the methoxy group and the hydrogen atom of the imine bond (see Figure 12). This value is in reasonable agreement with the experimental activation energy determined for the sub-glass transition, although the experimental value is slightly higher, probably as a consequence of the interactions between different polymeric chains.

Furthermore, the assigned nature of the β relaxation might explain the decrease observed in the intensity of this relaxation when the copper(II) content increases. The copper(II) coordination center hinders the rotation around the nitrogen donor atoms and fixes the dihedral angle θ_2 of the coordinated units. Consequently, the number of contributing rotational groups decreases as the copper(II) content increases. The activation energy remains constant, within experimental error, except for DMB-20, in which a slight decrease is observed. In this

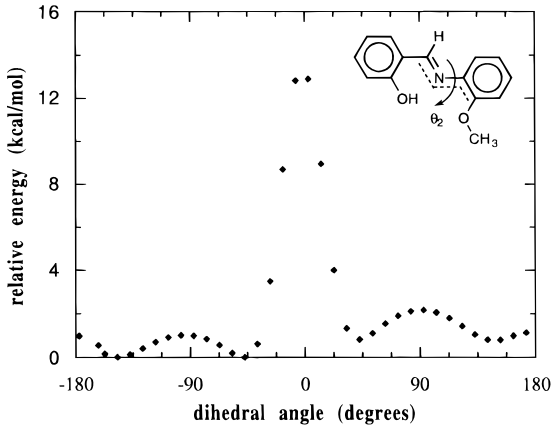

Figure 12. Relative energies as a function of dihedral angle θ_2 for *N*-(2-methoxyphenyl)salicylaldimine, which is a model of the mesogenic core. (Semiempirical calculations carried out by using the MOPAC-AM1 program.)

case, the higher copper(II) content might modify the region surrounding the noncomplexed mesogenic units, providing a higher separation between the neighboring polymeric chains and hence a decrease in intermolecular interactions.

As far as the character of the γ process is concerned, the preexponential factor, τ_∞, of the Arrhenius behavior obtained from the dielectric measurements gives values of around 10^{-13} s. This relaxation time is characteristic of an activated local motional relaxation. This is also supported by the high values of the shape parameter μ and their strong thermal variation from 0.75 at −150 °C to 0.50 at −70 °C, which suggests a broad distribution of the relaxation times. The values of the molar activation energy, 6.2−7.2 kcal/mol, are in agreement with the estimated value obtained from mechanical data for DMB-5 (7.4 kcal/mol). This relaxation can be tentatively assigned to local motions of the decamethylene flexible spacers connecting the mesogenic groups. The activation energy found experimentally for this process is lower than the similar γ relaxation of polyethylene (10−14 kcal/mol)[29] but higher than that found for polymers containing methylene sequences in lateral chains (5−6 kcal/mol).[30] Alternatively, rotational motions of the methoxy groups in the mesogenic units could explain the γ relaxation. However, the strength of this relaxation proved to be almost constant and independent of the cross-linking density, which suggests that the motions involved in the relaxation are not located in the mesogenic units.

Conclusions

The presence of two secondary sub-glass relaxations and a relaxation process associated with the T_g have been observed for the parent polymer, DMB, by dielectric spectroscopy (DS) and dynamic mechanical measurements (DMA). The β process has been associated with rotational motions within the rigid mesogenic units involving rotations around the nitrogen−phenyl ring bond. Semiempirical calculations gave rotational energy barriers similar to the activation energies obtained from DS and DMA. The γ process is attributed to the flexible spacer group. A new process is observed by DS at low frequency and has been analyzed in a complex electric modulus representation. The influence of the cross-linking degree on all these processes has been studied, although the influence on the α process is the most marked. Increases in the relaxation temperatures and strong decreases in the strength of the relaxation are observed as the copper(II) content increases. A WLF behavior is presented for the four compounds in the glass process.

Acknowledgment. This work is supported by the Comisión Interministerial de Ciencia y Tecnología of Spain (Project Nos. MAT94-0717-C02-01 and MAT94-0325-E). The authors also wish to acknowledge Dr. T. Sierra for help and suggestions on the computational calculations.

References and Notes

(1) See, for instance: (a) Biswas, A.; Gardner, K. H.; Wojtkoski, P. W. *Liquid Crystalline Polymers*; American Chemical Society: Washington, DC, **1990**; p 256. (b) Yang, C. J.; Jenekhe, S. A. *Chem. Mater.* **1991**, *3*, 878. (c) Yang, C. J.; Jenekhe, S. A.; Vanherzeele, H.; Meth, J. S. *Chem. Mater.* **1991**, *3*, 985. (d) Yang, C. J.; Jenekhe, S. A. *Chem. Mater.* **1994**, *6*, 196. (e) Yang, C. J.; Jenekhe, S. A. *Macromolecules* **1995**, *28*, 1180.
(2) Yang, H. H. *Aromatic High-Strength Fibers*; Wiley-Interscience: New York, 1989; p 641.
(3) (a) Barberá, J.; Oriol, L.; Serrano, J. L. *Liq. Cryst.* **1992**, *12*, 37. (b) Cerrada, P.; Oriol, L.; Piñol, M.; Serrano, J. L. *J. Polym. Sci., Polym. Chem.* **1996**, *34*, 2603.
(4) (a) Meléndez, E.; Serrano, J. L. *Mol. Cryst. Liq. Cryst.* **1983**, *91*, 173. (b) Elguero, J.; Jaime, C.; Marcos, M.; Meléndez, E.; Sánchez-Ferrando, F.; Serrano, J. L. *J. Mol. Struct.* **1987**, *150*, 1.
(5) Cerrada, P.; Oriol, L.; Piñol, M.; Serrano, J. L.; Iribarren, I.; Muñoz Guerra, S. *Macromolecules* **1996**, *29*, 2515.
(6) Chen, H.; Archer, R. D. *Macromolecules* **1996**, *29*, 1957.
(7) De, B. B.; Lohray, B. B.; Sivaram, S.; Dhal, P. K. *Macromolecules* **1994**, *27*, 1291.
(8) (a) Oriol, L.; Alonso, P. J.; Martínez, J. I.; Piñol, M.; Serrano, J. L. *Macromolecules* **1994**, *27*, 1869. (b) Alonso, P. J.; Martínez, J. I.; Oriol, L.; Piñol, M.; Serrano, J. L. *Adv. Mater.* **1994**, *6*, 663.
(9) Oriol, L.; Serrano, J. L. *Adv. Mater.* **1995**, *7*, 348.
(10) Haws, C. M.; Clark, M. G.; Attard, G. S. *Side Chain Liquid Crystal Polymers*; McArdle, C. B., Ed.; Blackie: Glasgow, 1989; p 196.
(11) Marcos, M.; Oriol, L.; Serrano, J. L.; Alonso, P. J.; Puértolas, J. A. *Macromolecules* **1990**, *23*, 5187.
(12) Puértolas, J. A.; Oriol, L.; Díaz-Calleja, R. *J. Non-Cryst. Solids* **1994**, *172*−174, 950.
(13) Wiesemann, A.; Zentel, R.; Lieser, G. *Acta Polym.* **1995**, *46*, 25.
(14) Morgan, P. W.; Kwolek, S. L.; Pletcher, T. C. *Macromolecules* **1987**, *20*, 729.
(15) Barberá, J.; Cerrada, P.; Oriol, L.; Piñol, M.; Serrano, J. L.; Alonso, P. J. *Liq. Cryst.*, in press.
(16) Marcos, M.; Oriol, L.; Serrano, J. L. *Macromolecules* **1992**, *25*, 5362.
(17) Starkweather, H. W. *Macromolecules* **1990**, ***23***, 328.
(18) Puértolas, J. A.; Díaz-Calleja, R.; Oriol, L. *Polymer* **1995**, *36*, 4579.
(19) Jonscher, A. K. *Universal Relaxation Law*; Chelsea Dielectrics Press: London 1996.
(20) Ross McDonald, J. *Impedance Spectroscopy*; Wiley: New York 1987.
(21) Williams, M. L.; Landel, R.; Ferry, J. D. *J. Am. Chem. Soc.* **1955**, *77*, 3701.
(22) Díaz-Calleja, R.; Sanchis, M. J.; Reis-Nunes, R. C.; Pinto, M.; Riande, E. *J. Appl. Phys.* **1995**, *78*, 1906.
(23) Havriliak, S.; Negami, S. *Polymer* **1967**, *8*, 161.
(24) Floudas, G.; Placke, P.; Stepanek, P.; Brown, W.; Fytas, G.; Ngai, K. L. *Macromolecules* **1995**, *28*, 6799.
(25) Alvarez, F.; Colmenero, J.; Wang, C. H.; Xia, J. L.; Fytas, G. *Macromolecules* **1995**, *28*, 6488.
(26) Elguero, J.; Jaime, C.; Marcos, M.; Meléndez, E.; Sánchez-Ferrando, F.; Serrano, J. L. *J. Mol. Struct.* **1987**, *150*, 1.
(27) Dewar, M. J. S.; Zoebisch, E. G.; Healy, E. F.; Stewart, J. J. P. *J. Am. Chem. Soc.* **1985**, *107*, 3902.
(28) Coburn, J. C.; Soper, P. D.; Auman, B. C. *Macromolecules* **1995**, *28*, 3253.
(29) Aschcraft, C. R.; Boyd, R. H. *J. Polym. Sci. Polym. Phys. Ed.* **1976**, *24*, 2153.
(30) Ribes, M.; Díaz-Calleja, R.; Gargallo, L.; Radic, D. *Polymer* **1991**, *32*, 2755.

MA961119O